Adaptive Mesh Simulations of Pellet Injection in Tokamaks

Ravi Samtaney

Computational Plasma Physics Group

Princeton Plasma Physics Laboratory

Princeton University

NERSC NUG Meeting, September 17, 2007

Oakland, CA

PPPL PRINCETON PLASMA PHYSICS LABORATORY

BERKELEY LAB

Pellet Injection: Motivation & Processes

- Motivation
  - *Injection of frozen hydrogen pellets is a viable method of fueling a tokamak*
  - *Presently there is no satisfactory simulation or comprehensive predictive model for ITER*
  - *Ratio of pellet size to device size is ~O(10^{-3})*

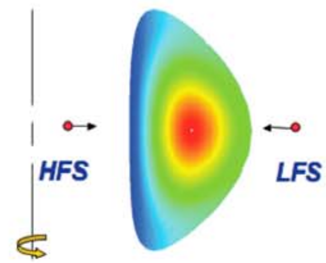

- Pellet-plasma interactions:
  - *Ablation: Considered well-understood*
  - *Mass deposition: Large scale MHD driven but not-so-well understood*
- Physical Processes
  - *Non-local electron transport along field lines rapidly heats the pellet cloud (τ_e).*
    - *Frozen pellet encounters hot plasma and ablates rapidly*
    - *A high β "plasmoid" is created*
  - *Ionized plasmoid expands*
  - *Fast magnetosonic time scale τ_f.*
  - *Pellet mass moves across flux surfaces τ_a.*
    - *So-called "anomalous" transport across flux surfaces*
  - *Pellet cloud expands along field lines τ_c.*
    - *Pellet mass distribution continues along field lines until press. equilibration*
  - *Pellet lifetime τ_p*

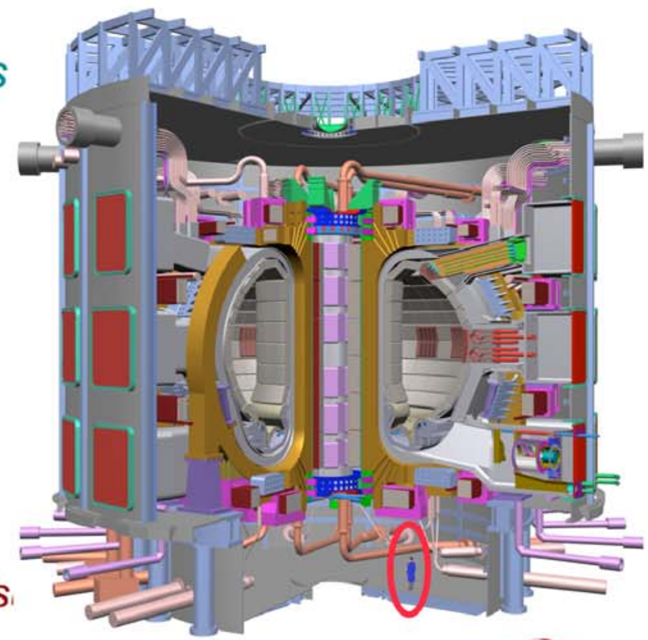

Numerical Challenges & Resolution Requirements

- Time Scales $\tau_e < \tau_f < \tau_a < \tau_c < \tau_p$
- Spatial scales: Pellet radius r_p << Device size L ~O(10^{-3})
- Presence of magnetic reconnection
  - *Thickness of resistive layer scales with ~ $\eta^{1/2}$*
  - *Time scale for reconnection is ~ $\eta^{-1/2}$*
- Pellet cloud density ~ O(10^4) times ambient plasma density
- Electron heat flux is non-local
- Large pressure and density gradients in the vicinity of cloud
- Pellet lifetime ~ O(10^{-3}) s → long time integrations

Resolution estimates

Tokamak	Major Radius	N	N_{steps}	Spacetime Points
CDXU (Small)	0.3	2×10^7	2×10^5	4×10^{12}
DIIID (Medium)	1.75	3.3×10^9	7×10^6	2.3×10^{17}
ITER (Large)	6.2	1.5×10^{11}	9×10^7	1.4×10^{19}

MHD Primer

- A continuum or fluid description of a plasma
  - *A hierarchy of MHD models can be derived from Fokker-Planck equations*
  - *Single fluid resistive MHD derived*
    - *Assuming a "single fluid" and quasi-neutrality*
    - *High collisionality and small Larmour radius*
- MHD equations are mathematical models describing the flow of a conducting fluid coupled with electromagnetism
- Governing equations: hydrodynamics coupled with Maxwell's equations
  Faraday: $\partial \mathbf{B}/\partial t = -\nabla \times \mathbf{E}$ (implies $\nabla \cdot \mathbf{B}=0$)
  Ohm: $\mathbf{E}=-\mathbf{v} \times \mathbf{B} + \eta \mathbf{J}$
  Ampere: $\mathbf{J}=\nabla \times \mathbf{B}$

  Momentum equations include $\mathbf{J}\times \mathbf{B}$ force
  Energy equation includes $\mathbf{J} \cdot \mathbf{E}$ (Ohmic heating)
- Several ways to combine hydrodynamics with Maxwell
  - *Weakly coupled, strongly coupled, vector potential formulations etc.*
  - *Mathematically, the result is a system of coupled nonlinear partial differential equations which usually must be solved numerically*
  - *For ideal MHD the equations are hyperbolic PDEs*
  - *Numerically it is challenging to preserve the solenoidal property of the magnetic field*

PPPL PRINCETON PLASMA PHYSICS LABORATORY

BERKELEY LAB

Current Work

- Combine global MHD simulations in a tokamak geometry with detailed local physics including ablation, ionization and electron heating in the neighborhood of the pellet

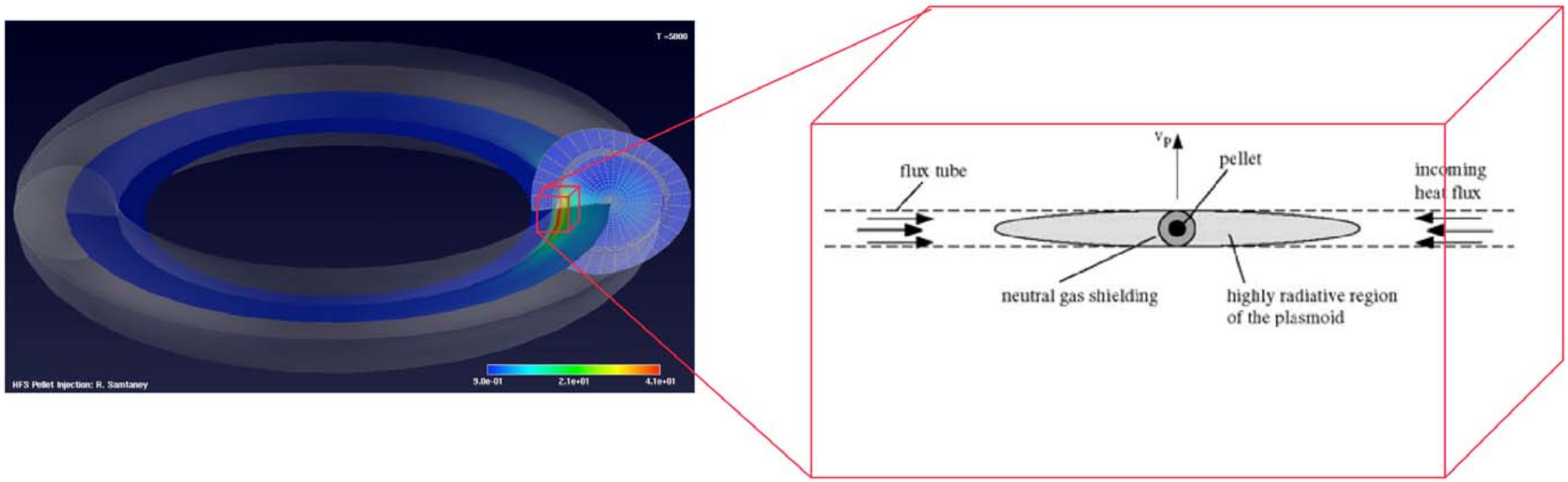

- AMR techniques to mitigate the complexity of the multiple scales in the problem
- Newton-Krylov approach for wide range of temporal scales (not discussed today)

Mathematical Model

- Single fluid resistive MHD equations in conservation form

$$\frac{\partial U}{\partial t} + \underbrace{\frac{1}{R}\frac{\partial RF}{\partial R} + \frac{\partial H}{\partial z} + \frac{1}{R}\frac{\partial G}{\partial \phi} = S}_{\text{Hyperbolic terms}} + \underbrace{\frac{1}{R}\frac{\partial RF_D}{\partial R} + \frac{\partial H_D}{\partial z} + \frac{1}{R}\frac{\partial G_D}{\partial \phi} + S_D}_{\text{Diffusive terms}} + \boxed{S_{pellet}}$$

Density: Ablation
Energy :Electron heat flux

$$U = \{\rho, \rho u_R, \rho u_\phi, \rho u_Z, B_R, B_\phi, B_Z, e\}^T$$

$$F \equiv F(U) = \begin{Bmatrix} \rho u_R \\ \rho u_R^2 + p_t - B_R^2 \\ \rho u_R u_\phi - B_R B_\phi \\ \rho u_R u_Z - B_R B_Z \\ 0 \\ u_R B_Z - u_Z B_R \\ u_R B_\phi - u_\phi B_R \\ (e+p_t)u_R - (B_k u_k) B_R \end{Bmatrix}, \qquad H \equiv H(U) = \begin{Bmatrix} \rho u_Z \\ \rho u_R u_Z - B_R B_Z \\ \rho u_Z u_\phi - B_Z B_\phi \\ \rho u_Z^2 + p_t - B_Z^2 \\ u_Z B_R - u_R B_Z \\ 0 \\ u_Z B_\phi - u_\phi B_Z \\ (e+p_t)u_Z - (B_k u_k) B_Z \end{Bmatrix},$$

$$G \equiv G(U) = \begin{Bmatrix} \rho u_\phi \\ \rho u_R u_\phi - B_R B_\phi \\ \rho u_\phi^2 + p_t - B_\phi^2 \\ \rho u_Z u_\phi - B_Z B_\phi \\ u_\phi B_R - u_R B_\phi \\ u_\phi B_Z - u_Z B_\phi \\ 0 \\ (e+p_t)u_\phi - (B_k u_k) B_\phi \end{Bmatrix}, \qquad S(U) = -\frac{1}{R}\begin{Bmatrix} 0 \\ B_\phi^2 - \rho u_\phi^2 - p_t \\ \rho u_R u_\phi - B_R B_\phi \\ 0 \\ 0 \\ 0 \\ 0 \\ u_\phi B_R - u_R B_\phi \end{Bmatrix}$$

- Additional constraint $\nabla \cdot \mathbf{B} = 0$

PPPL PRINCETON PLASMA PHYSICS LABORATORY

BERKELEY LAB

Electron Heat Flux Model

- Semi-analytical Model by Parks et al. (Phys. Plasmas 2000)
  - *Assumes Maxwellian electrons and neglects pitch angle scattering*

$$\boxed{-\nabla \cdot q_e = \frac{q_\infty n}{\tau_\infty}\left[g(u_+) + g(u_-)\right]}$$

$$q_\infty = \sqrt{\frac{2}{\pi m_e}} n_{e\infty} (k\, T_{e\infty})^{\frac{3}{2}} \quad \tau_\infty = \frac{T_{e\infty}^2}{8\pi e^4 \log \Omega} \quad g(u) = u^{\frac{1}{2}} K_1(u^{\frac{1}{2}})/4$$

$$u_\pm = \frac{\tau_\pm}{\tau_\infty} \qquad \tau_\pm = \pm \int_{\mp\infty}^{\boldsymbol{x}} n(s)ds$$

- Solve for opacities as a "steady-state" solution to an advection-reaction equation $\frac{d\tau}{ds} = n(\boldsymbol{x}) \qquad \hat{b} \cdot \nabla \tau = n(\boldsymbol{x})$
  - *Solve by using an upwind method*
    - *Advection velocity is **b***

$$\boxed{\frac{d\tau}{d\zeta} + \hat{\boldsymbol{b}} \cdot \nabla \tau = n(\boldsymbol{x})}$$

Curvilinear coordinates for shaped plasma

- Adopt a flux-tube coordinate system (flux surfaces ψ are determined from a separate equilibrium calculation)
  - $R \equiv R(\xi, \eta)$, and $Z \equiv Z(\xi, \eta)$
  - $\xi \equiv \xi(R,Z)$, and $\eta \equiv \eta(R,Z)$
  - ϕ coordinate is retained as before

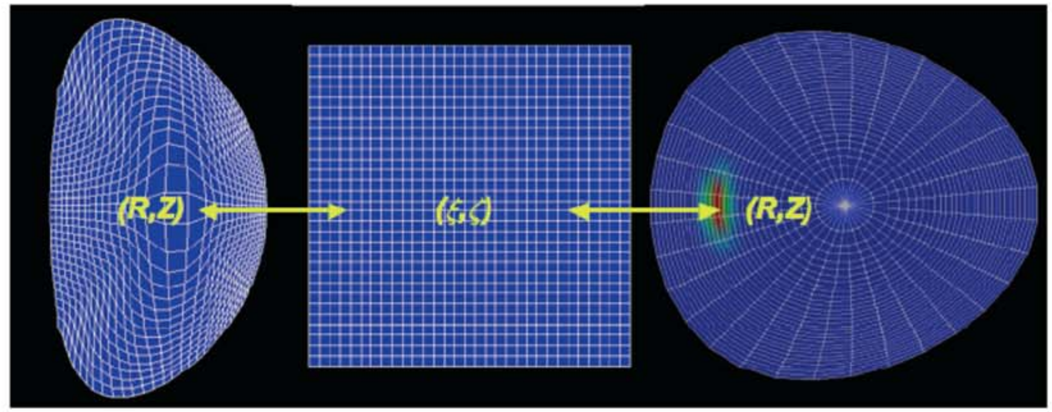

- Equations in transformed coordinates

$$\frac{\partial UJ}{\partial t} + \frac{1}{R}\frac{\partial R\tilde{F}}{\partial \xi} + \frac{1}{R}\frac{\partial R\tilde{H}}{\partial \eta} + \frac{1}{R}\frac{\partial \tilde{G}}{\partial \phi} = \tilde{S}\,.$$

$$\tilde{H} = J(\eta_R F + \eta_z H) = -z_\xi F + R_\xi H,$$

$$\tilde{F} = J(\xi_R F + \xi_z H) = z_\eta F - R_\eta H,$$

$$\tilde{G} = JG, \qquad \tilde{S} = JS.$$

Numerical method

- Finite volume approach
- Explicit second order or third order TVD Runge-Kutta time stepping
- The hyperbolic fluxes are evaluated using upwinding methods
  - *seven-wave Riemann solver:* $F \equiv F(U_L, U_R) = \frac{1}{2}(F(U_L) + F(U_R) - \sum_k \alpha_k \mid \lambda_k \mid r_k)$ where $\alpha_k = l_k (U_R - U_L)$
  - *Harten-Lee-vanLeer (HLL) Method* (SIAM Review 1983)
    $F \equiv F(U_L, U_R) = \lambda_{min} F(U_L) + \lambda_{max} F(U_R) + \lambda_{min} \lambda_{max} (U_R - U_L) / (\lambda_{max} - \lambda_{min})$
- Diffusive fluxes computed using standard second order central differences
- Imposing the solenoidal condition on B is important
- **Initial Conditions:** Express $B = 1/R(\phi \times \nabla \psi + g(\psi)\, \phi) \neq fnc(\phi)$. Initial state is an MHD equilibrium obtained from a Grad-Shafranov solver.
- **Boundary Conditions**: Perfectly conducting BCs; periodic in ϕ.

PPPL PRINCETON PLASMA PHYSICS LABORATORY

BERKELEY LAB

Adaptive Mesh Refinement with Chombo

- ***Chombo*** is a collection of C++ libraries for implementing block-structured adaptive mesh refinement (AMR) finite difference calculations (http://www.seesar.lbl.gov/ANAG/chombo)
  - *(Chombo is an AMR developer's toolkit)*
- Adaptivity in both space and time
- Mesh generation: necessary to ensure volume preservation and areas of faces upon refinement
- Flux-refluxing step at end of time step ensures conservation

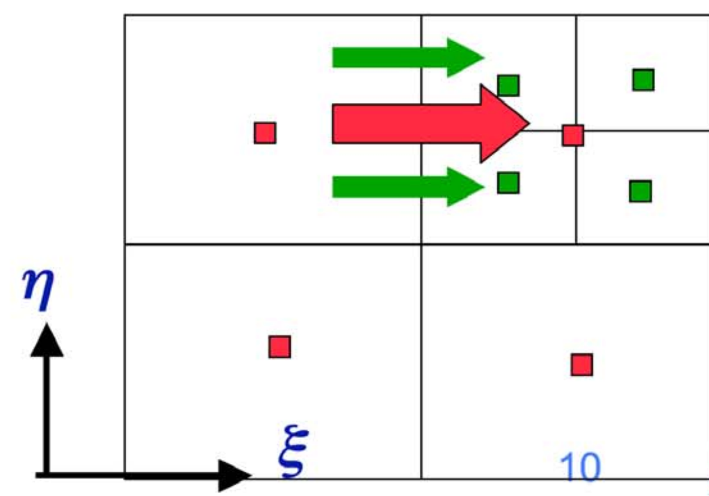

PPPL PRINCETON PLASMA PHYSICS LABORATORY

BERKELEY LAB

Pellet Injection: AMR

- Meshes clustered around pellet
- Computational space mesh structure shown on right
- Mesh stats
  - *32^3 – base mesh with 5 levels, and refinement factor 2*
  - *Effective resolution: 1024^3*
  - *Total number of finite volume cells:113408*
  - *Finest mesh covers 0.015 % of the total volume*
  - *Time adaptivity:*
    $1\ (\Delta t)_{base} = 32\ (\Delta t)_{finest}$

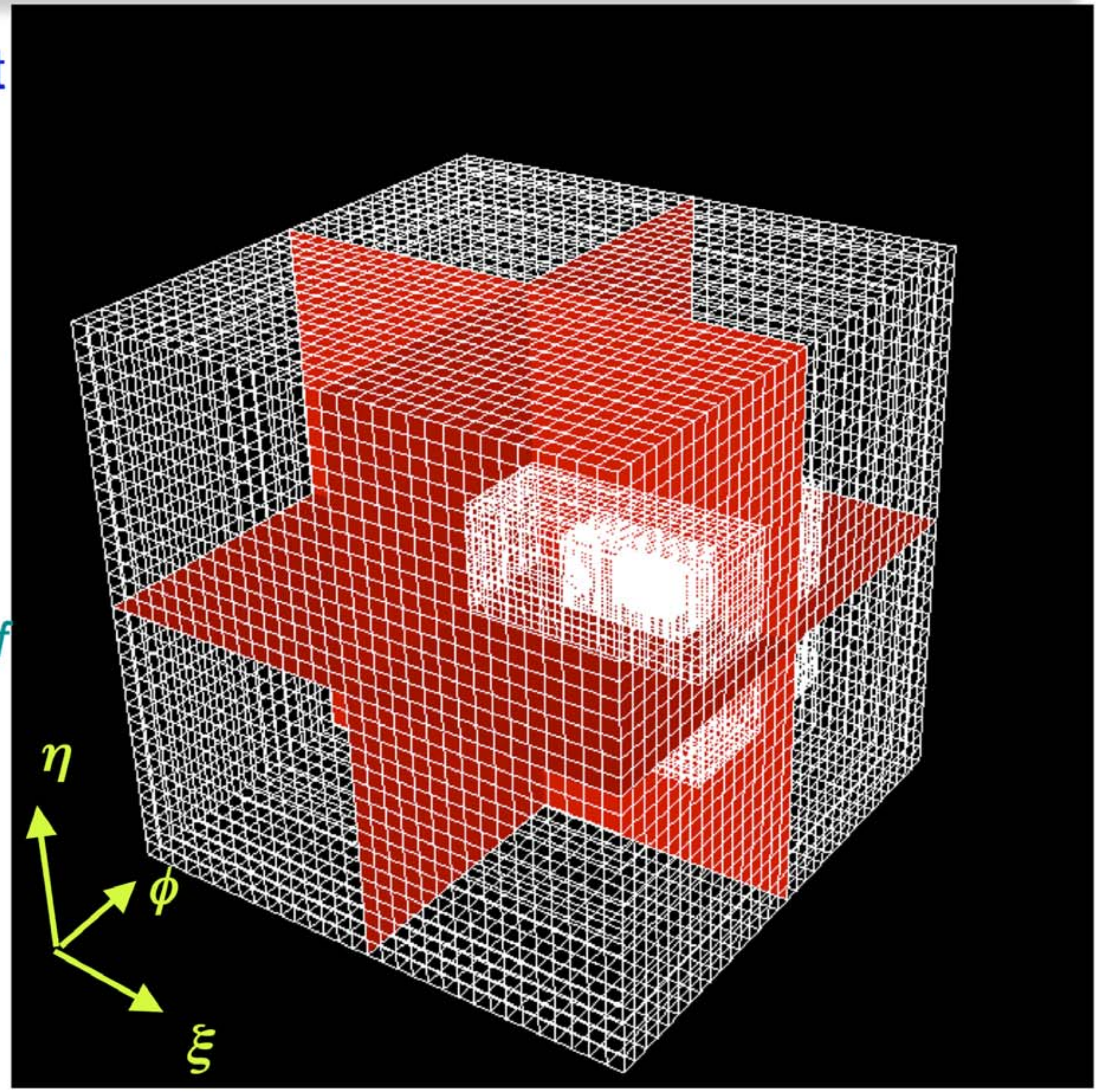

Pellet Injection: Zoom into Pellet Region

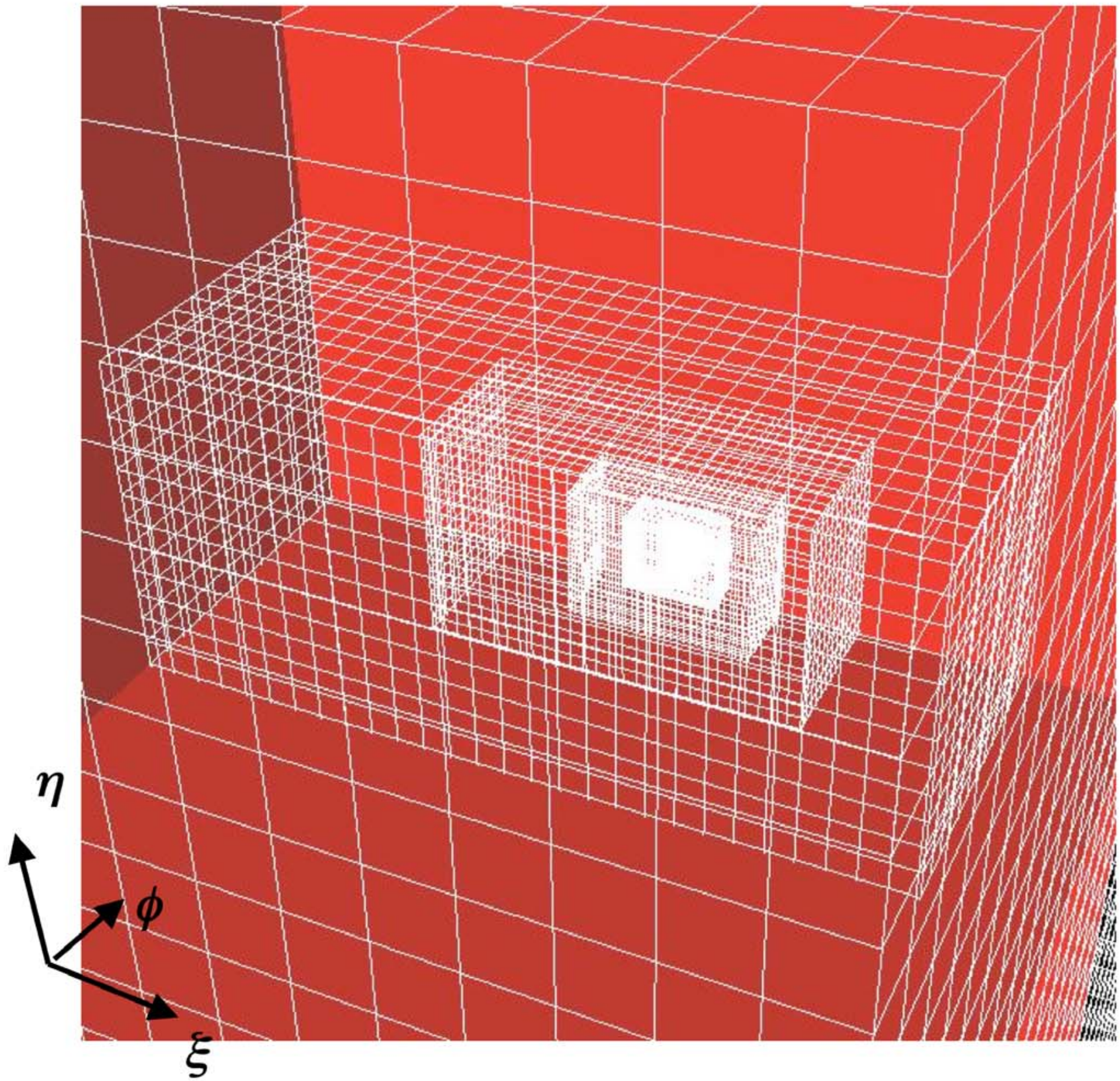

PPPL PRINCETON PLASMA PHYSICS LABORATORY

BERKELEY LAB

Pellet Injection: Zoom in

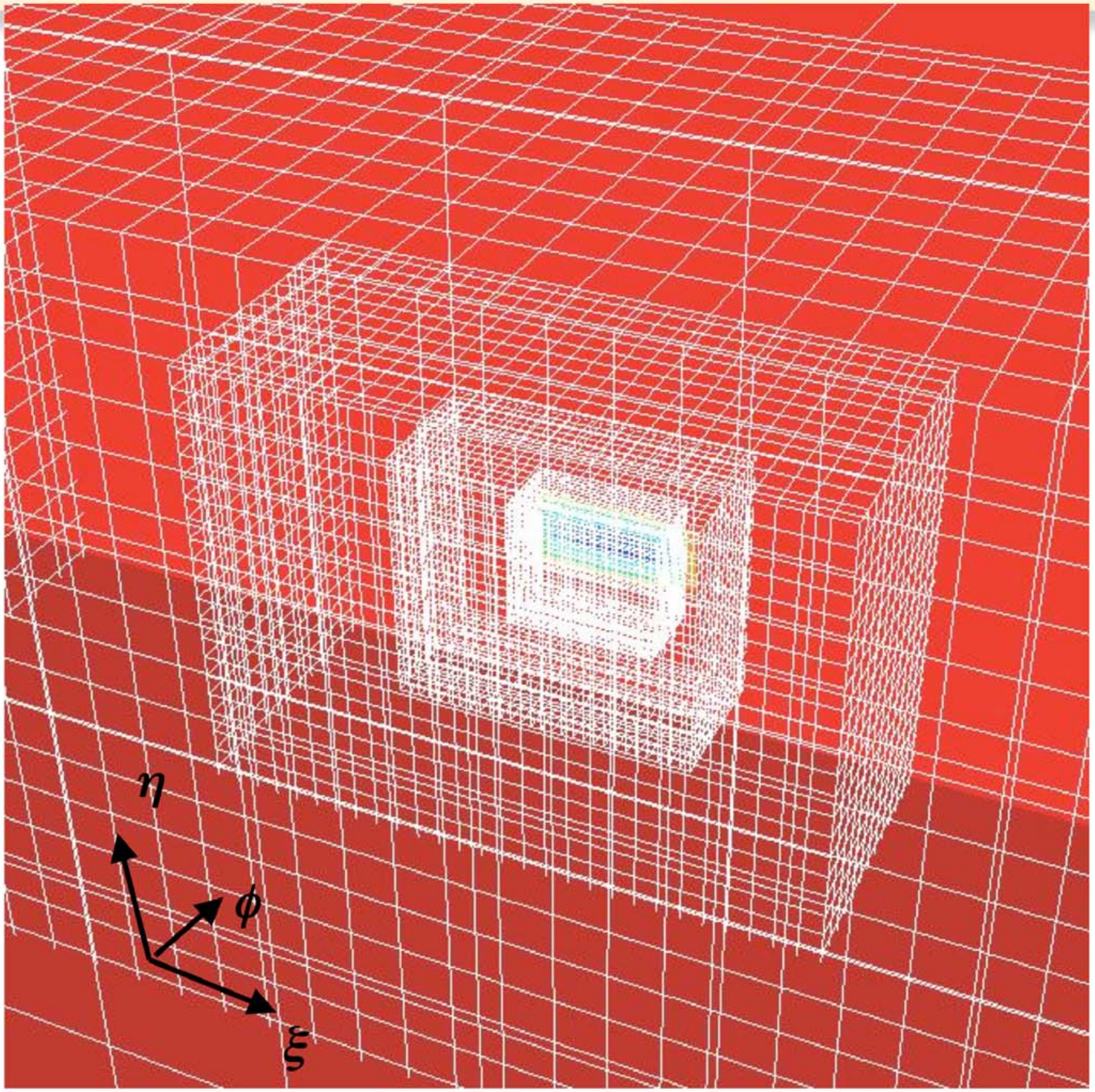

Pellet Injection: Pellet in Finest Mesh

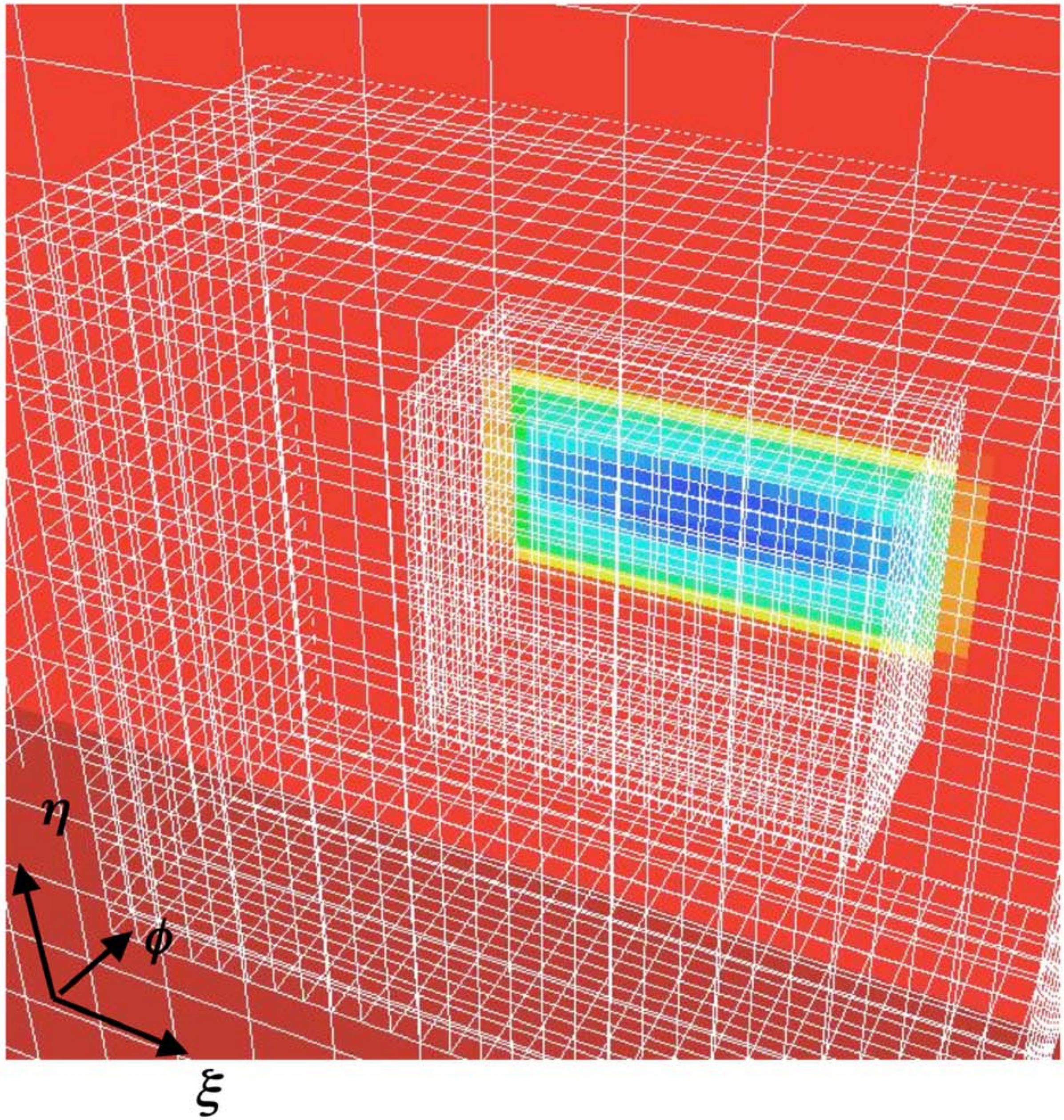

Pellet Injection: Pellet Cloud Density

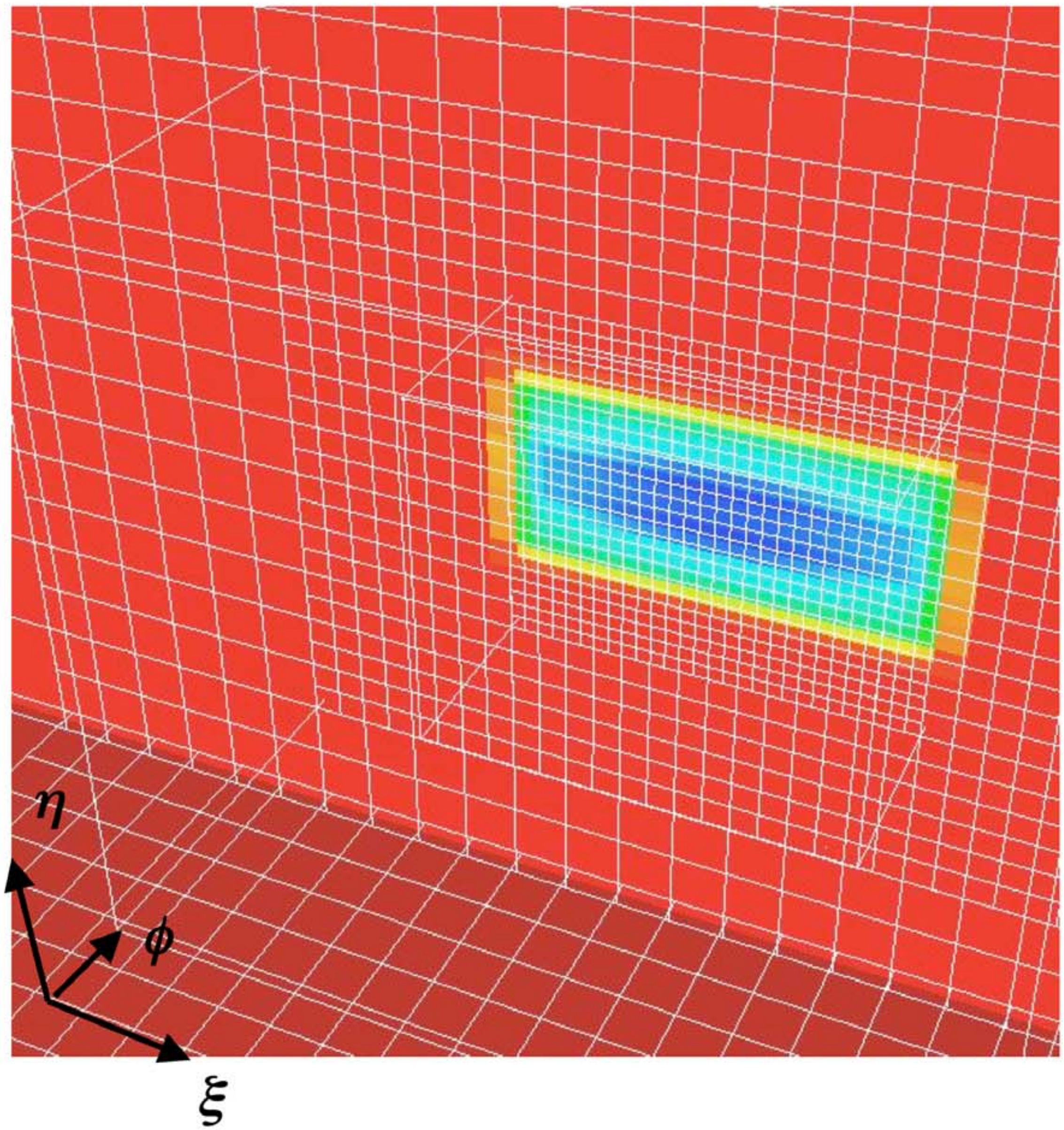

Results - HFS vs. LFS

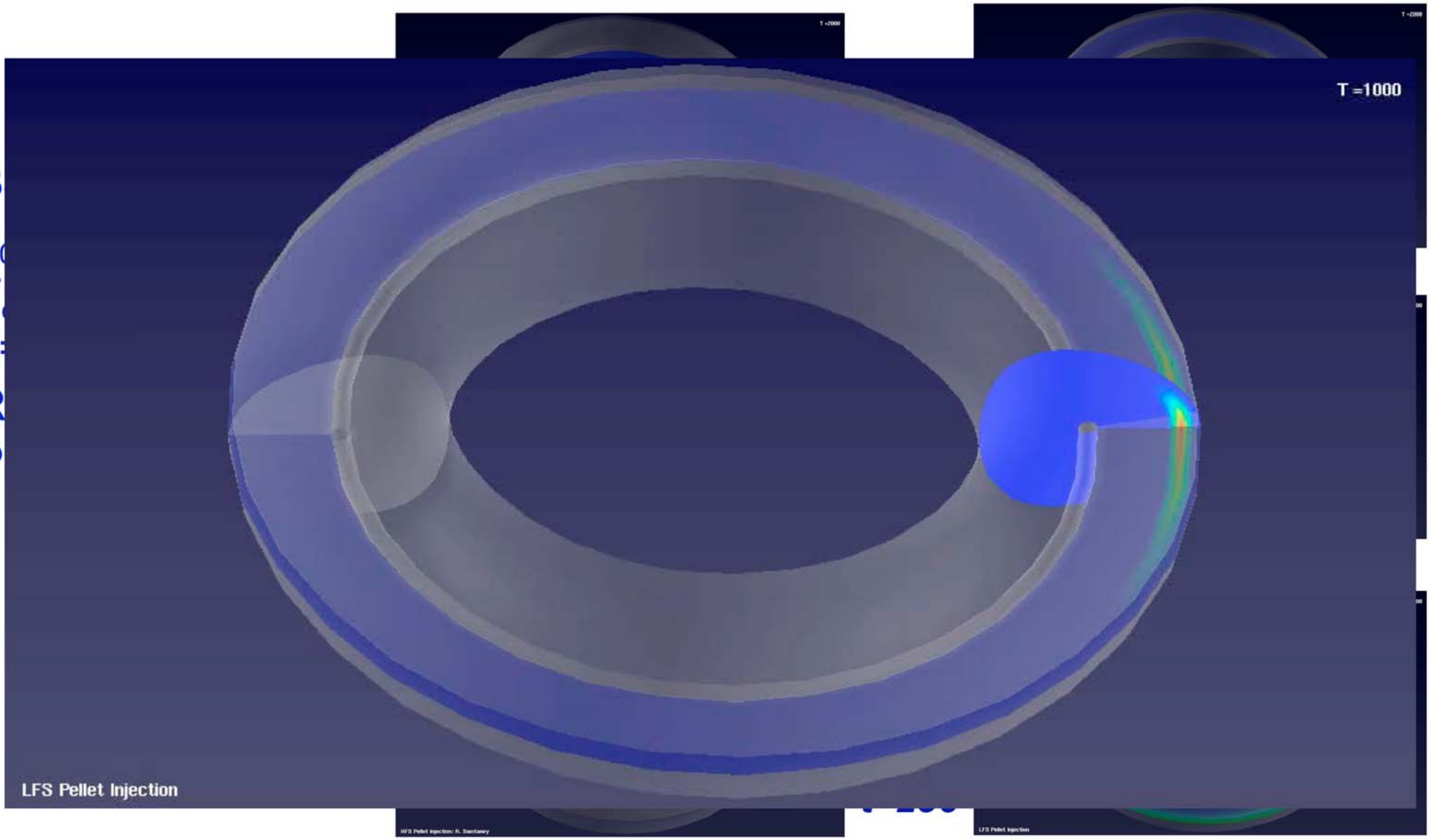

Results - HFS vs. LFS

B
n
T
β
R
P

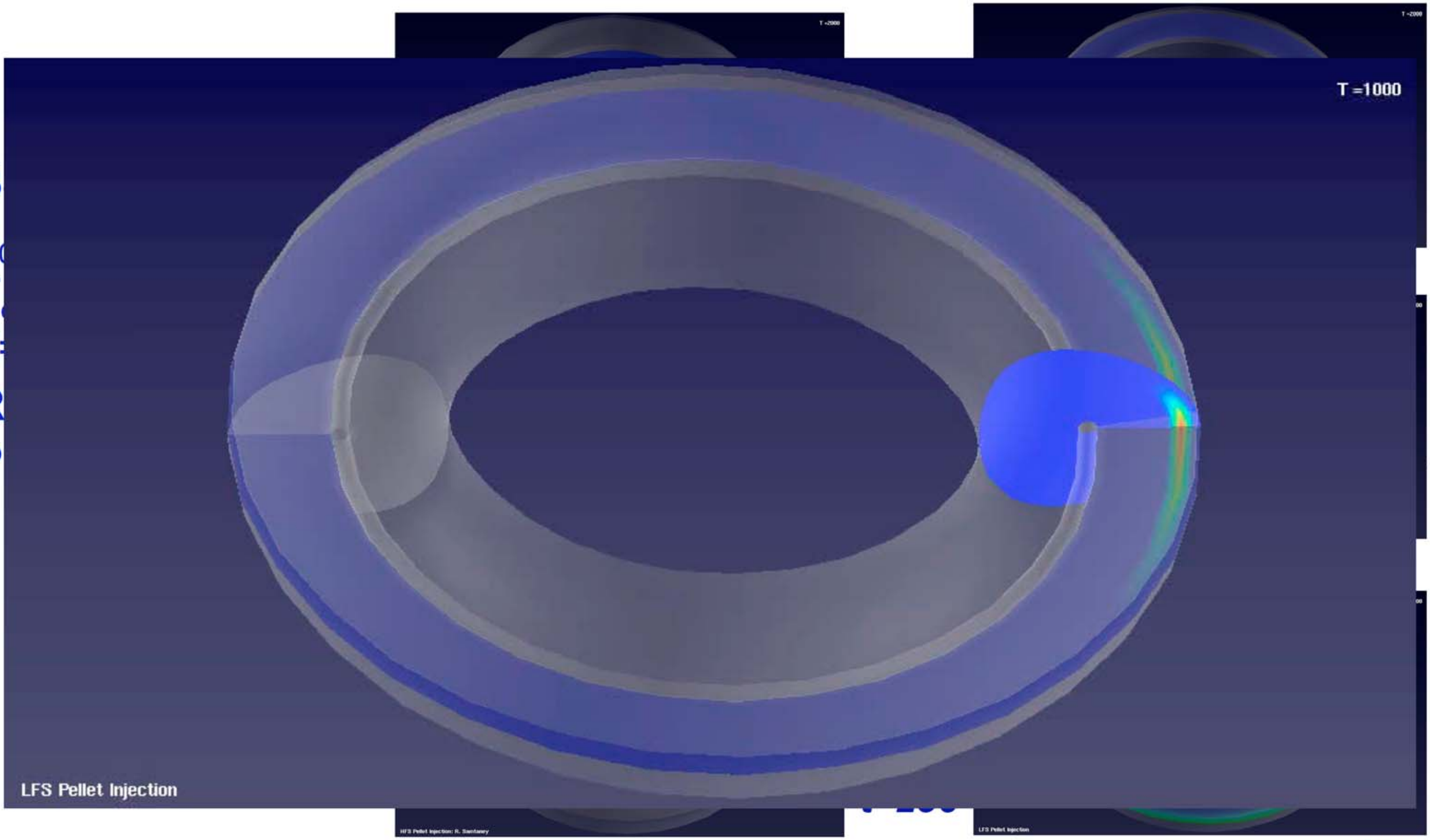

Results - HFS vs. LFS

B_T = 0.375T
n_0=1.5× $10^{19}/m^3$
$T_{e\infty}$=1.3Kev
β=0.05
R_0=1m, a=0.3 m
Pellet: r_p=1mm,
v_p=1000m/s

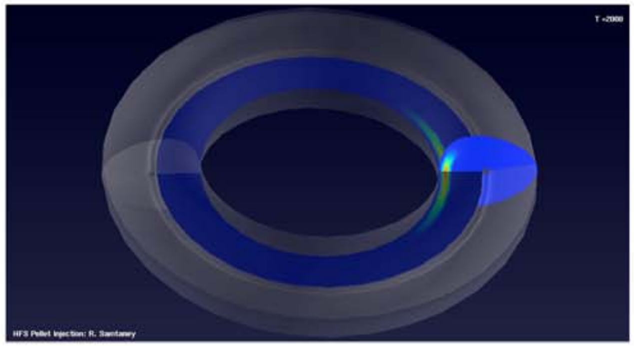

t=7

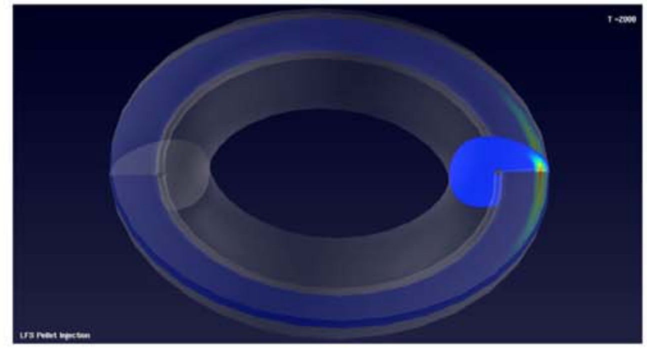

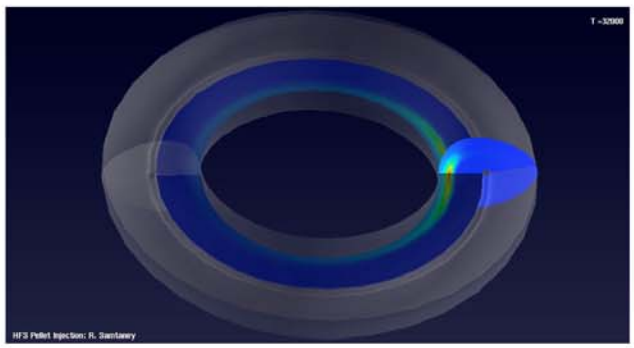

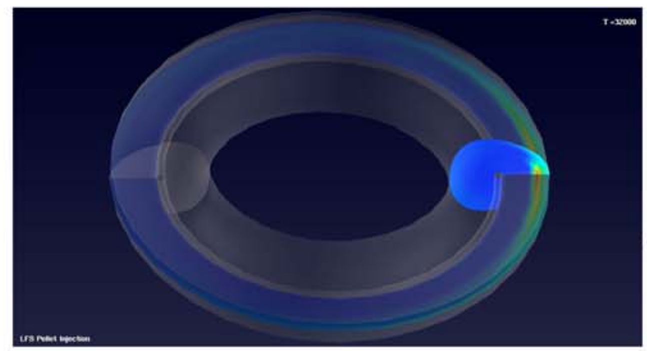

ρ

t=100

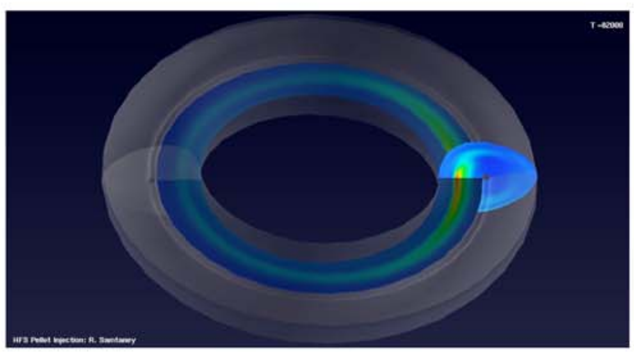

t=256

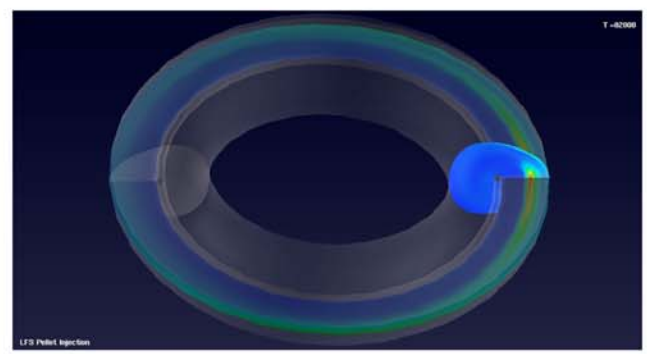

Results - HFS vs. LFS

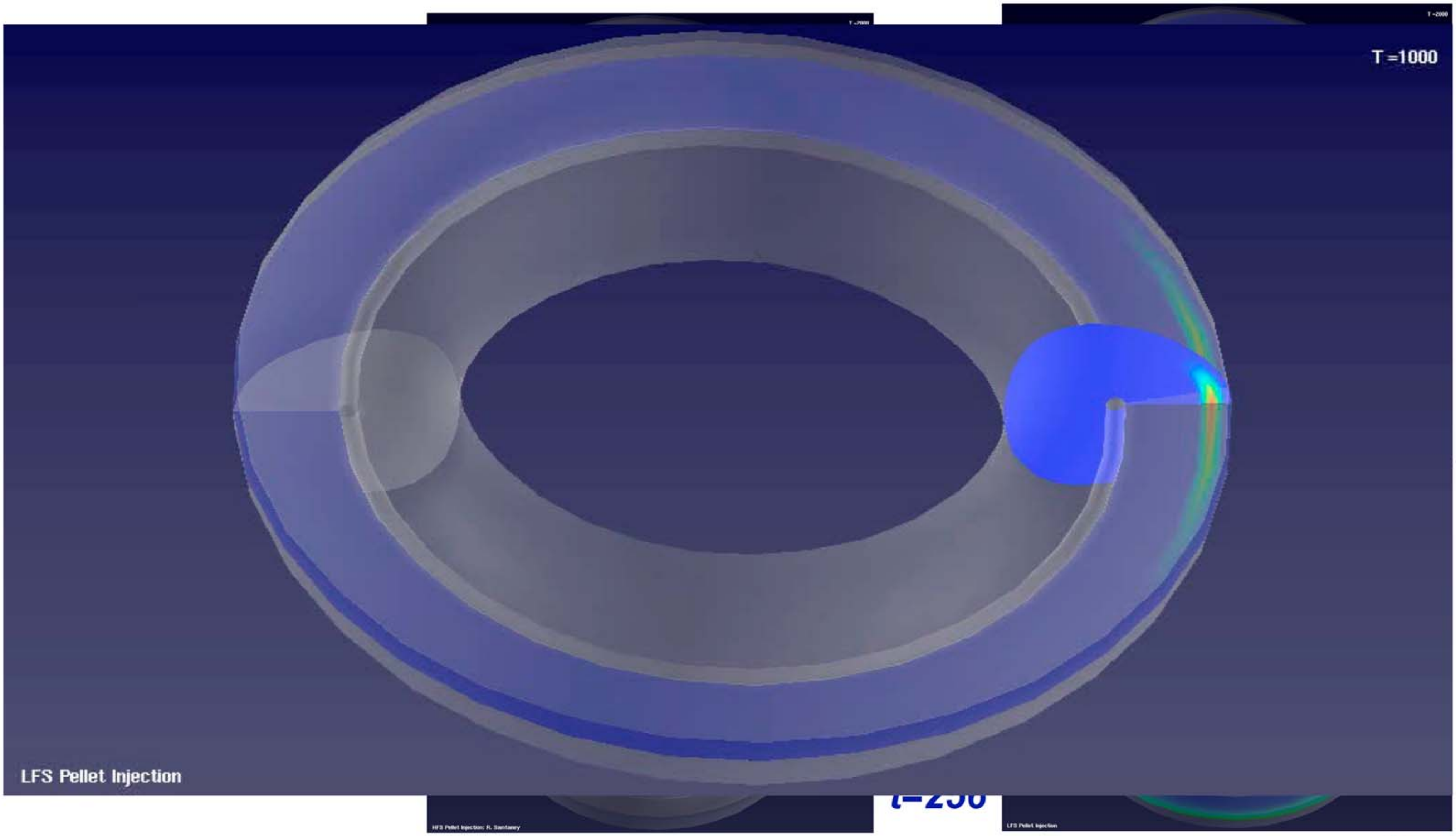

HFS vs. LFS - Average Density Profiles

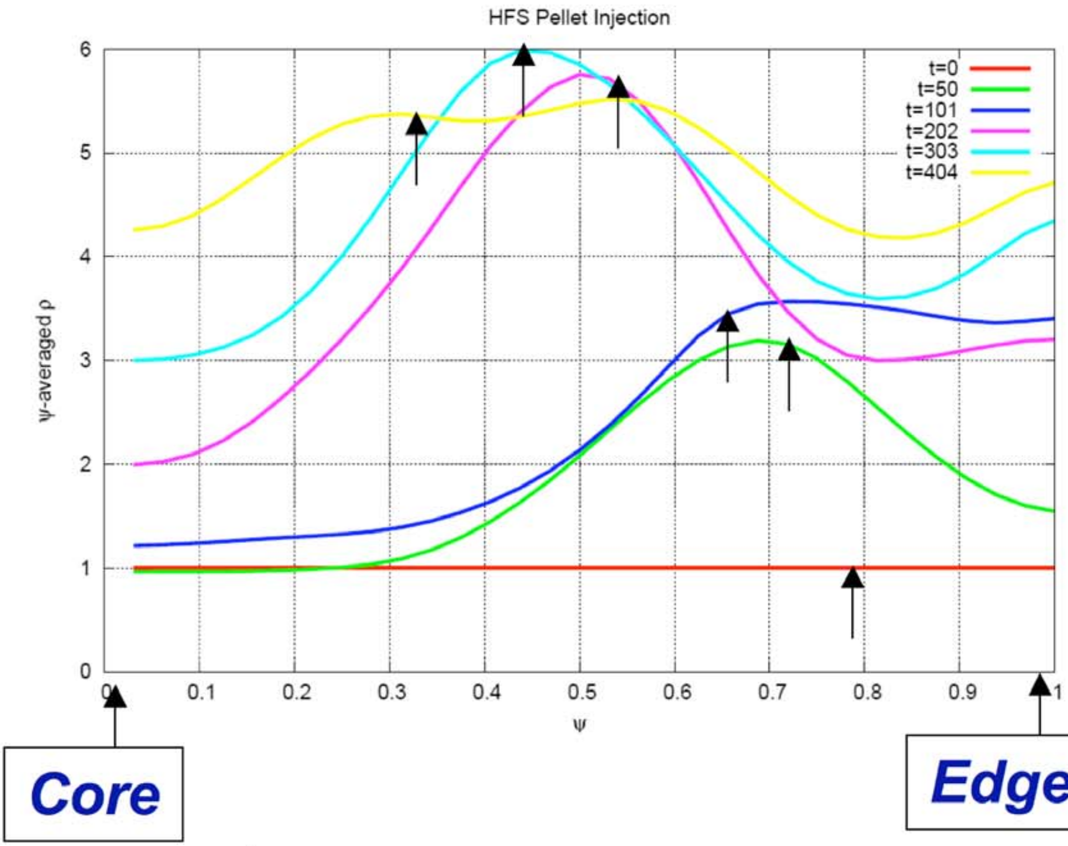

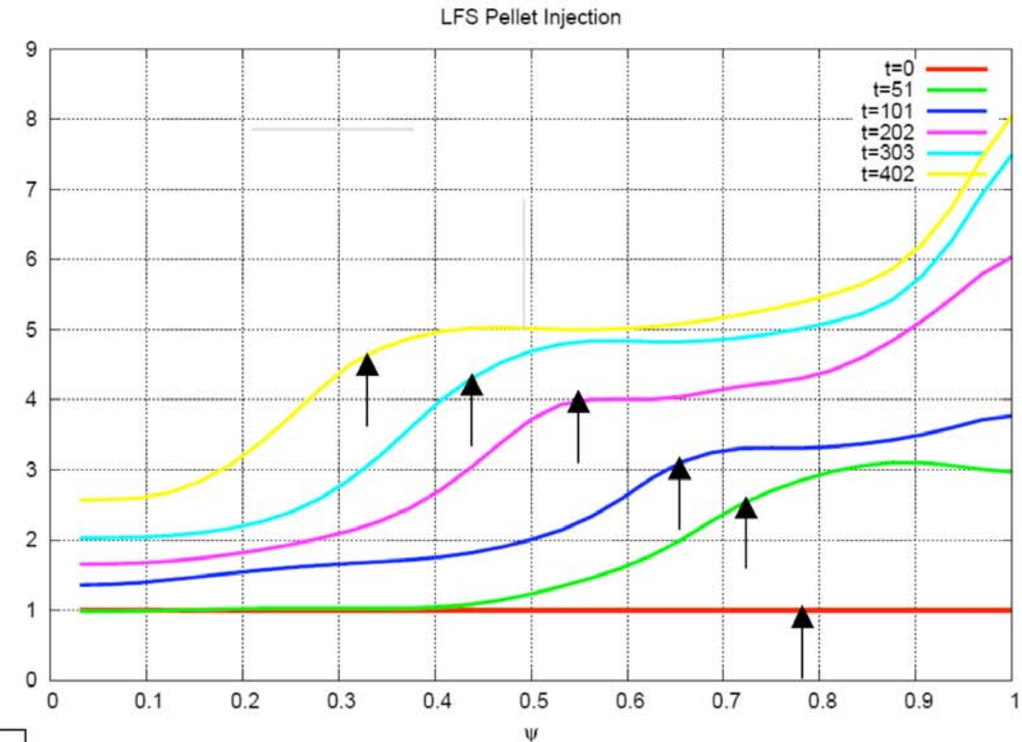

HFS Pellet injection shows better core fueling than LFS

Arrows indicate average pellet location

Most likely explanation: Nonlinear manifestation of an MHD interchange instability.

Pellet Injection: LFS/HFS Launch

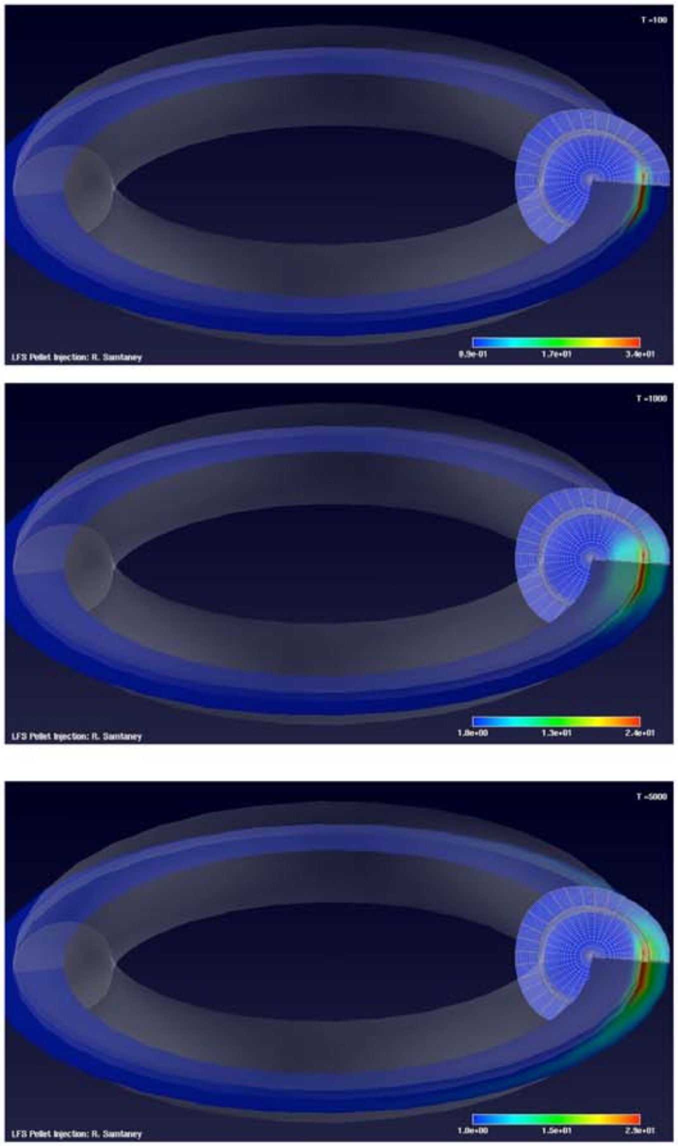

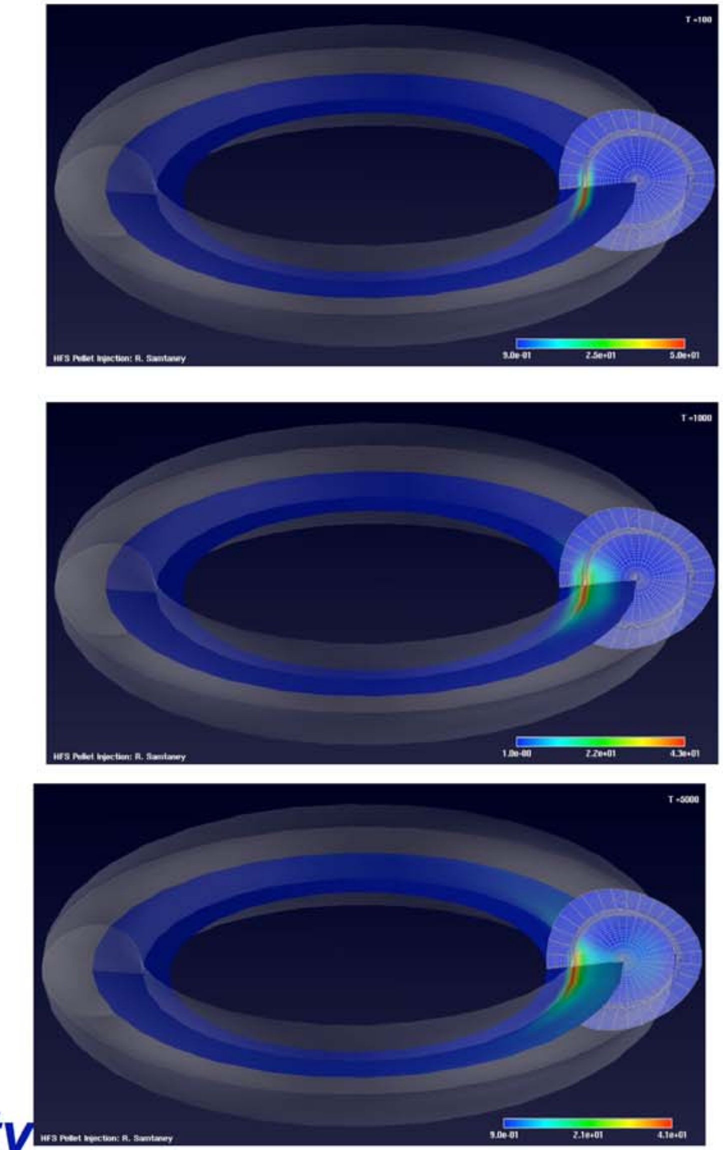

Density

AMR Programming Model

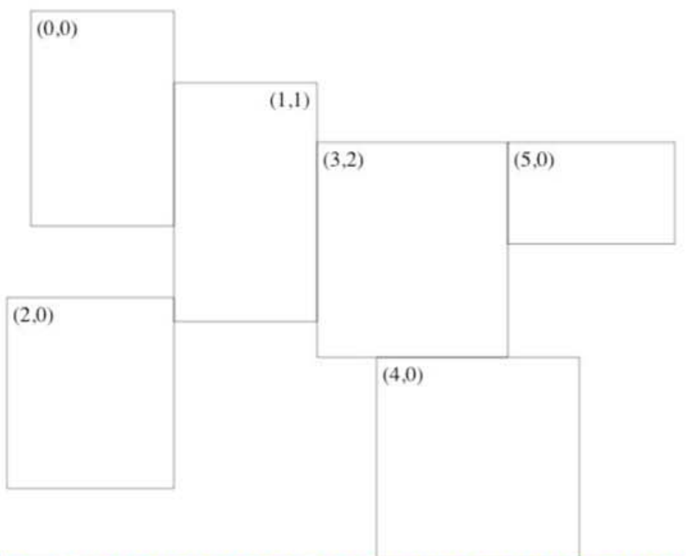

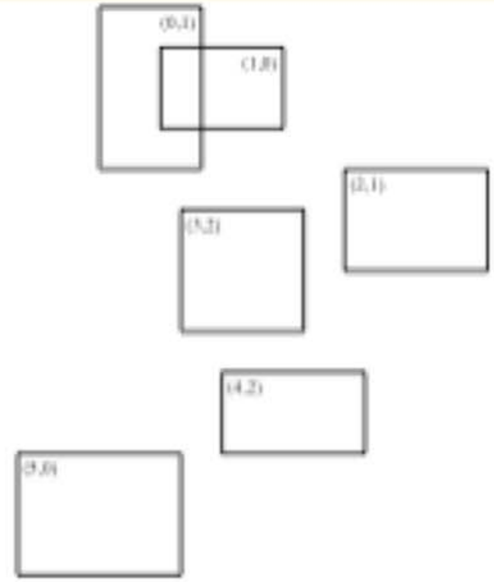

- Domain decomposition that assigns rectangular patches to processors. All processors have access to processor assignment metadata. Distributed grid data built on top of these metadata.
- Local computation: iterate over patches owned by processor. Processor has access only to local data.
- Communication primitives: exchange of ghost cell data, copying from a disjoint union of rectangles to some other union of rectangles.
- Interlevel operations: interpolating boundary data, averaging / interpolation between levels combine communication and irregular computation.

PPPL PRINCETON PLASMA PHYSICS LABORATORY

BERKELEY LAB

Defining Scalability, Performance

- Operator peak performance: maximum performance for evaluating an operator on a uniform grid on a single processor. For stencil operations, this has been typically 10%-20% of the nominal peak. We assess performance in terms of a fraction of operator peak performance.
- Adaptivity factor: ratio of the time to perform the calculation on a uniform grid at the finest resolution to the time to solution for the AMR calculation. The former is generally estimated from smaller runs and assuming perfect weak scaling, rather than computed directly.
- Implementation efficiency: what fraction of time is spent on regular computation (e.g. in Fortran77 or other optimized single-patch operations). For the examples described here, implementation efficiency is very close to the fraction of operator peak performance.

PPPL PRINCETON PLASMA PHYSICS LABORATORY

BERKELEY LAB

AMR Gas Dynamics Benchmark

- Unsplit PPM solver - 6K flops / grid point to update a cell. Explicit method, so ghost cell values copied / interpolated only once per update. Easiest case.
- Single image is a spherical shock tube in 3D, with finest grids covering a spherical shell. Two levels of refinement, factor of 4 each. Refinement in time proportional refinement in space. Fixed-sized (16x16x16) patches. Five unknowns / cell, 62M grid points, with1B grid point updates performed per coarse time step.
- Operator peak performance on XT4 is 530 Mflops / processor.
- Timing only the update step - no initialization, regridding, etc.
- Results obtained with hyperbolic code “out of the box” from Chombo distribution.
- 96% efficient scaled speedup over range of 128-8192 processors (173-181 seconds).
- Fraction of operator peak: 85% (450 Mflops / processor).
- Adaptivity factor: 16.

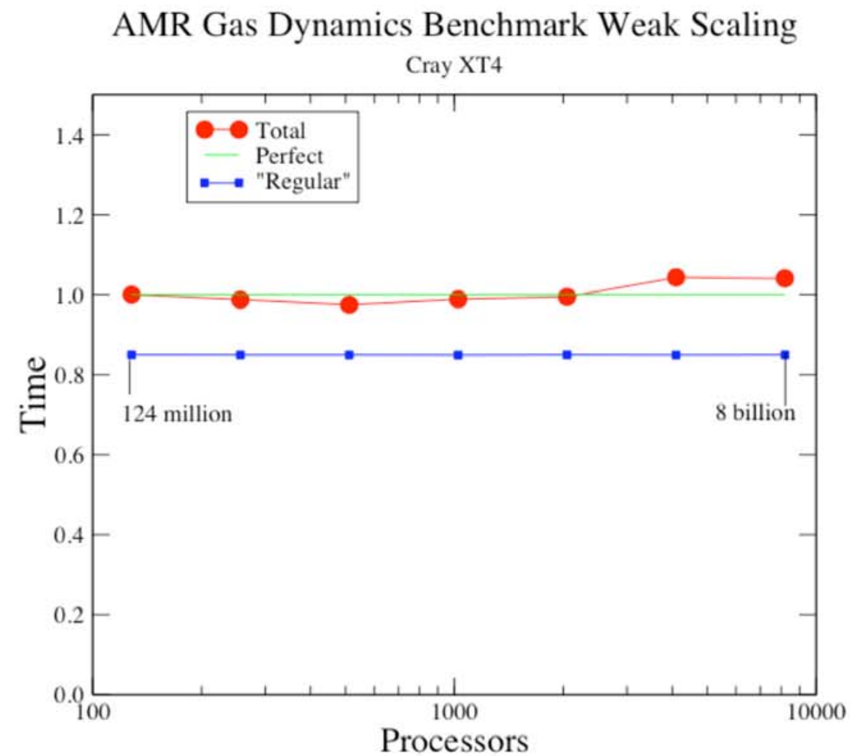

Scaling of AMR for explicit methods is relatively easy.

Slide: Courtesy P. Colella, APDEC, LBNL

AMR Poisson Benchmark

- Multilevel discretization of Laplacian, with AMR multigrid algorithm used as solver. 10 iterations of AMR-MG V-cycle = 1700 Flops / grid point. Over 100 calls to communication (exchange / copyTo) per iteration. Typical of broad range of elliptic solvers on AMR grids.
- Single image is two rings. Two levels of refinement, factor of 4 each. Patch size is allowed to vary between 8^3 and 32^3. One unknown per cell, total of 15M grid points per image.
- Operator peak performance on XT4 is 840 Mflops / processor.
- Timing only the solver - no initialization.
- Results obtained after significant effort in code optimization (2 months), leading to 10X improvement in per-processor performance and in scalability.
- 87% efficient scaled speedup over range of 256-8192 processors (8.4-9.5 seconds).
- Fraction of operator peak: 45% (375 Mflops / processor).
- Adaptivity factor: 48 (estimated).

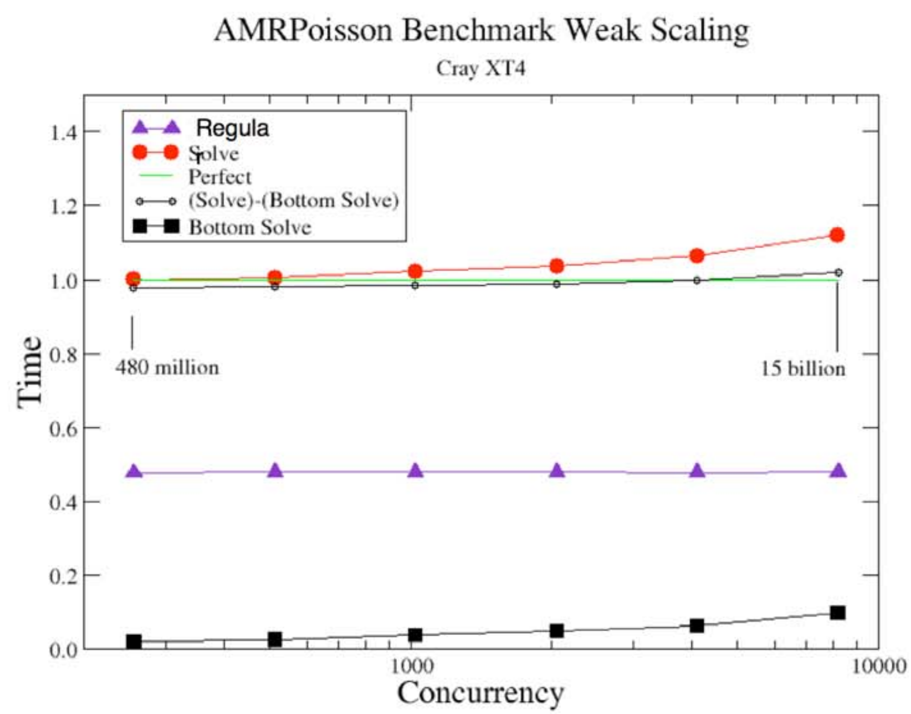

Development of scalable Poisson solvers is one of the most challenging goals for AMR.

Slide: Courtesy P. Colella, APDEC, LBNL

Conclusion

- Developed a finite volume upwind adaptive curvilinear mesh MHD code for pellet injection including kinetic-based model for electron heat flux
- Simulations show better core fueling for HFS injection than LFS, in qualitatively agreement with experiments
  - *Adaptivity factor estimated for these simulations ~ 100-200*

- Future Work
  - *Implicit treatment (explicit too slow)*
  - *solvers which can handle large anisotropies, large variations in plasma properties, curvilinear meshes*
  - *Optimize to 1000s of processors (translating the success of benchmark suites to the pellet code)*
  - *Validation against experiment*
  - *Visualization & data analysis (analytics)*

Acknowledgement

- P. Colella and Applied Numerical Algorithms Group (APDEC, LBNL)
- S. C. Jardin (CEMM, PPPL)
- D. Reynolds (UCSD, TOPS), C. Woodward (LLNL, TOPS)
- Funded through the TOPS, CEMM and APDEC SciDAC Centers. RS supported by US DOE Contract No. DE-AC020-76-CH03073
- This research used resources of the National Energy Research Scientific Computing Center, which is supported by the Office of Science of the U.S. Department of Energy under Contract No. DE-AC03-76SF00098.

PPPL PRINCETON PLASMA PHYSICS LABORATORY

BERKELEY LAB